LASER INTERFEROMETER GRAVITATIONAL WAVE OBSERVATORY
- LIGO -
CALIFORNIA INSTITUTE OF TECHNOLOGY
MASSACHUSETTS INSTITUTE OF TECHNOLOGY

Document Type	**LIGO-T95000x-xx - Cxx**	02/03/97

Beam Tube Dynamics

S. Chatterji and R. Weiss

Distribution of this draft:

xyz

This is an internal working note
of the LIGO Project..

California Institute of Technology
LIGO Project - stS 51-33
Pasadena CA 91125
Phone (818) 395-2129
Fax (818) 304-9834
E-stail: info@ligo.caltech.edu

stassachusetts Institute of Technology
LIGO Project - stS 20B-145
Castbridge, stA 01239
Phone (617) 253-4824
Fax (617) 253-7014
E-stail: info@ligo.stit.edu

WWW: http://www.ligo.caltech.edu/

SUMMARY

Measurements of the motion of the beam tube at the Washington site were made to refine the estimates of the phase noise due to scattering. The measurements indicate:

1) The beamtube is primarily driven by acoustic excitation rather than seismic noise.

2) Both measurements and finite element modeling show the beam tube to be a complex multimode mechanical oscillator with closely spaced (3 to 5 Hz) normal modes. The system is more simply described as an acoustic transmission line than as a lumped element mechanical system.

3) Under quiet conditions (winds less than 5 mph and all rotating machinery at the site turned off), the broad band displacement spectrum ($f < 100Hz$) of the covered beamtube at a fixed support exceeds the LIGO standard spectrum by a factor of 3 to 10 and by factors of 30 to 100 in high Q transmission modes of the beam tube. The motions are correlated with acoustic pressure fluctuations and not seismic motions

4) The beam tube motions at a point half way between the fixed and compliant support is larger by factors of 2 to 3 than motion at a fixed support.

5) The prior estimates of beam tube motion used in the initial calculations for the scattering noise power in the beam tube need to be multiplied by factors of 3 to 10 for quiet conditions at the site and, furthermore by an additional factor of the square of the wind velocity ratio for average conditions at the site (another factor of 2 to 4). The assumption is that the dominant acoustic noise on the beam tube comes from wind induced acoustic excitations transmitted through the beam tube enclosure.

6) The acoustic coupling to the beam tube will be reduced by the thermal insulation applied for the bakeout. The insulation will provide acoustic isolation at frequencies above 200 Hz but is not expected to provide attenuation at frequencies below 100Hz.

7) It would be useful to directly measure the 10 to 200 Hz acoustic noise spectrum in the beam tube enclosure over a range of wind conditions at the site.

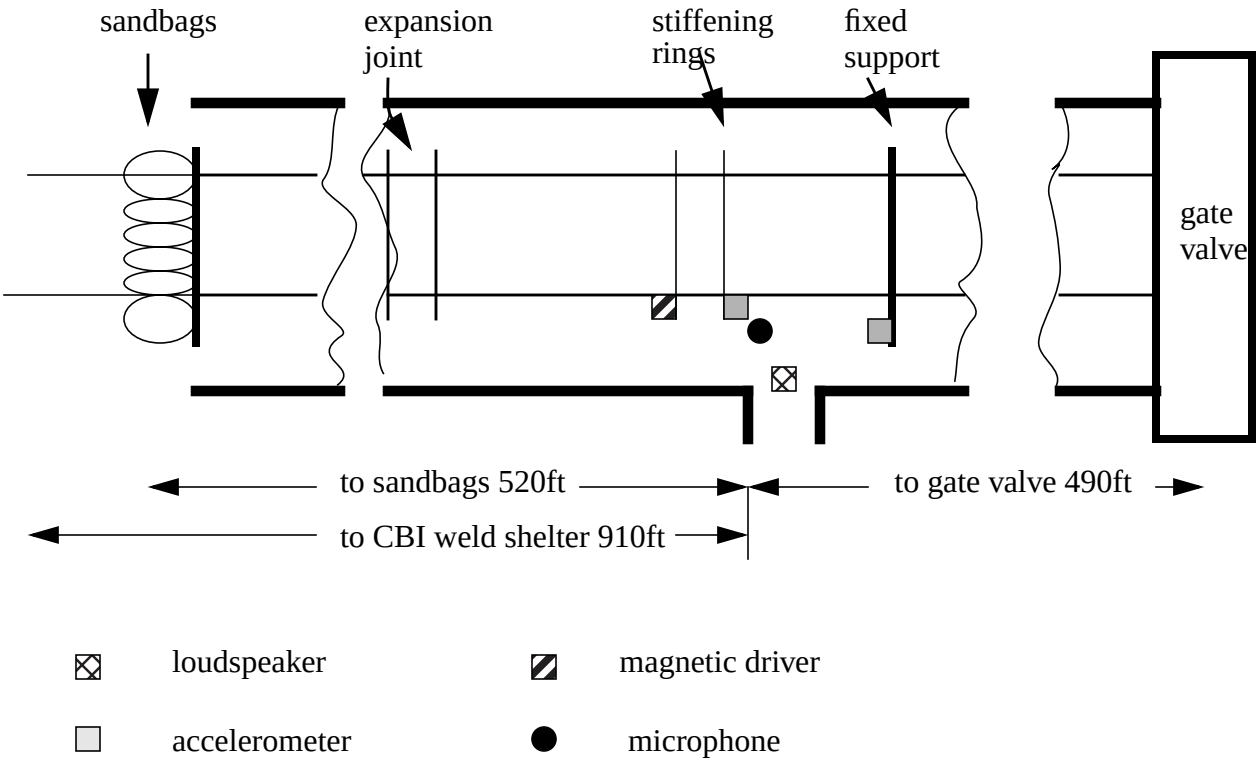

Figure 1 Schematic of the experimental arrangement

INTRODUCTION. The measurements, made between January 30 through February 1, 1997, included:

1) A sampling of the acceleration power spectrum in the vertical, horizontal, and longitudinal directions of the tube at a fixed support ring, at a stiffening ring 10 meters from the fixed support and at the base of the fixed support where it attaches to the concrete slab. These measurements were made after dark with all CB&I rotating machinery off under low wind conditions and with the instruments powered by batteries.

2) A measurement of the acoustic transfer function of vertical, horizontal and longitudinal acceleration response to acoustic excitation derived from a loudspeaker monitored by a microphone in proximity to the accelerometer. The loudspeaker was mounted in one of the doors of the beam tube enclosure. The excitation was a chirped sinusoid.

3) Measurement of the transient response of the tube at a stiffening ring 10m from the fixed support. The measurements consisted of the horizontal spectrum after a horizontal impulse at the fixed support, the vertical spectrum after a vertical impulse and the longitudinal spectrum after a longitudinal impulse.

4) Measurement of the acceleration to applied force transfer function for horizontal acceleration from horizontal excitation, and longitudinal acceleration from longitudinal excitation. The excita-

tion was derived from a magnet attached to the beam tube driven by an oscillating current in a coil mounted to the ground. The excitation was a chirped sinusoid.

The experimental arrangement is schematized in Figure 1. The beam tube cover extends from the gate valve to the sandbags placed on the tube, a distance of about 1000 ft. The sandbags were intended to attenuate the propagation of wind induced excitations on the uncovered part of the tube to the measurement region. The gaps in the beam tube enclosure between sections as well as at their join to the slab were filled by flexible polyethane rope to reduce wind induced acoustic coupling to the tube. The sealing was done for approximately 180 ft on either side of the measurement area. The instrumentation was setup near one of the safety escape doors in the beam tube enclosure approximately in the middle of the covered section. The door could be covered by a plywood sheet.

Measurements were carried out after CB&I had stopped construction for the day. Critical low noise measurements were taken with all CB&I rotating equipment turned off (pumps and air conditioning fans, beam tube air distribution system), the measurement equipment was battery powered and during conditions with winds under 5 mph. The power to the CB&I equipment (lighting, heaters, instrumentation,etc) was not turned off since the perturbation to the measurements was manageable and would have caused delays in construction activities on the crew's return in the morning. The spectral features at 60 Hz and multiples in the high sensitivity acceleration power spectra are due to mechanical excitation of the slab and tube by vibrating transformers 1000 ft from the measurement region. The less critical measurements were made with AC power provided by a portable generator placed 100ft from the door outside the beam tube enclosure.

The instrumentation consisted of high sensitivity PZT accelerometers coupled to low noise preamplifiers operating at the thermal noise limit, Stanford Instrument bandpass intermediate amplifiers, a storage oscilloscope and a portable (battery operable) Hewlett Packard dynamic signal analyser. The data was observed during the measurements and recorded for analysis on floppy disks. (The use of the Stanford Instrument amplifiers, storage oscilloscope and the loan of the HP dynamic signal analyser were arranged by Rick Savage.) Additional instrumentation consisted of a PZT microphone and various acoustic and mechanical drivers to stimulate the tube.

Acceleration spectra on the beam tube. Figures 2, 3 and 4 show the acceleration noise in $\frac{g}{\sqrt{\text{Hz}}}$ on the beam tube under quiet conditions at the site. The legend in all the figures is the same. The dashed curve at the bottom is the instrument noise which begins to encroach on the measurement below 10 Hz. The next higher curve shows the noise on the fixed support at the intersection with the concrete slab. The 60, 120, 180 and 300 Hz peaks come from mechanical motions imparted to the beam tube and slab by magnetostriction in the transformers in the CB&I buildings. The broadband noise agrees with Rohay's seismic measurements for quiet conditions below 100Hz. Above 30 Hz the seismic noise is about a factor 10 to 20 lower in amplitude than the LIGO standard spectrum (shown as a dashed line in the figures). The spectrum using a solid line is from an accel

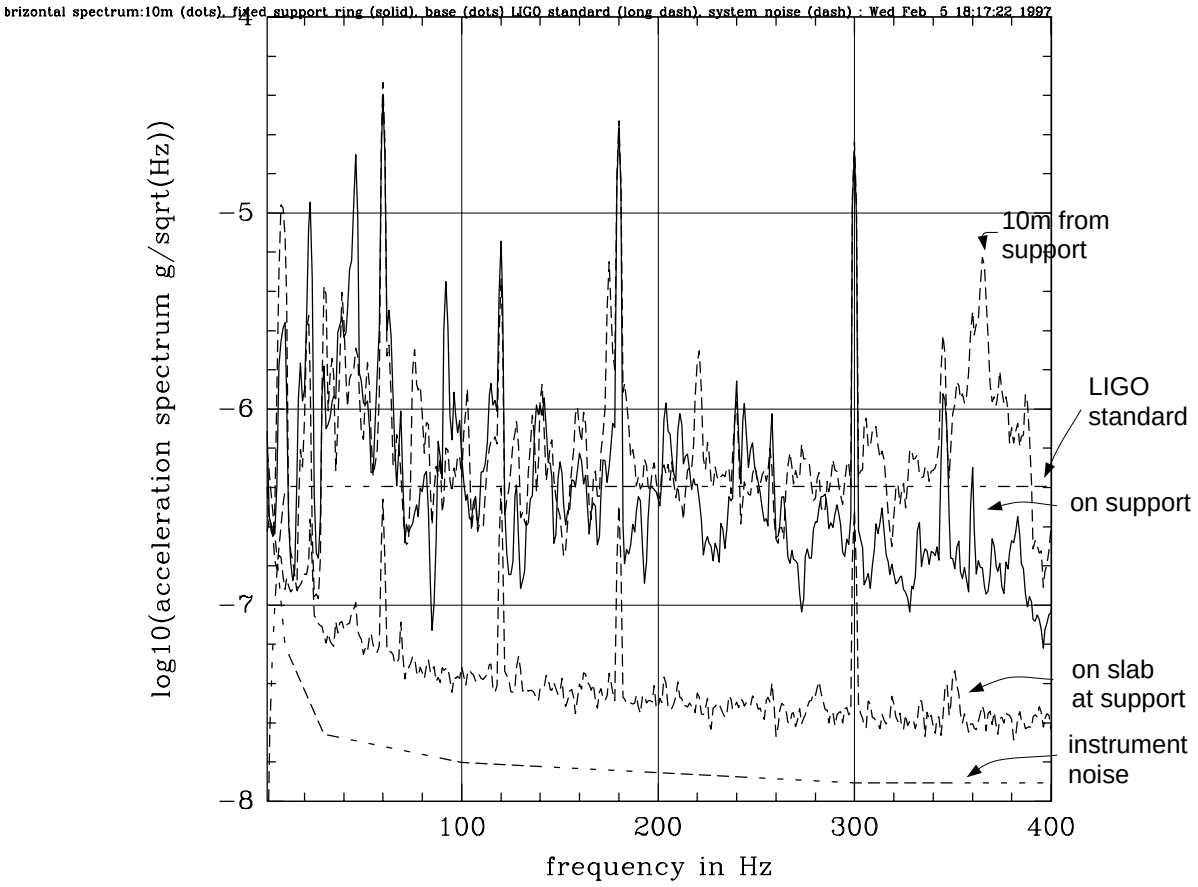

Figure 2 Horizontal acceleration spectrum

rometer mounted on the support ring associated with the fixed support. This is the location for most of the baffles, especially those near the middle of the tube. The spectrum is dominated by closely spaced narrow spectral lines with Q larger than 100 but generally less than 600. The same lines are seen in driven and transient spectra shown in subsequent figures and in table 1. The spectrum plotted in dots is taken at a stiffening ring 10 meters from the fixed support, about half way between the fixed and flexible support. This shows larger motions at some of the normal modes and a general tendency to be more easily excited than the region at the support in the 300 to 400 Hz band which includes the radial stiffening ring modes.

The horizontal motions were always measured on a horizontal diameter of the tube, the vertical measurements at the top of the tube and longitudinal measurements at a point on the horizontal diameter. The apparatus cross coupling of the three directions due to accelerometer imperfections and mounting block errors was less then 0.5%.

The tube motions are largest in the horizontal direction where the broadband motion is between 3 to 10 times larger than the standard LIGO spectrum and the amplitude in several normal modes 30 to 100 times larger.

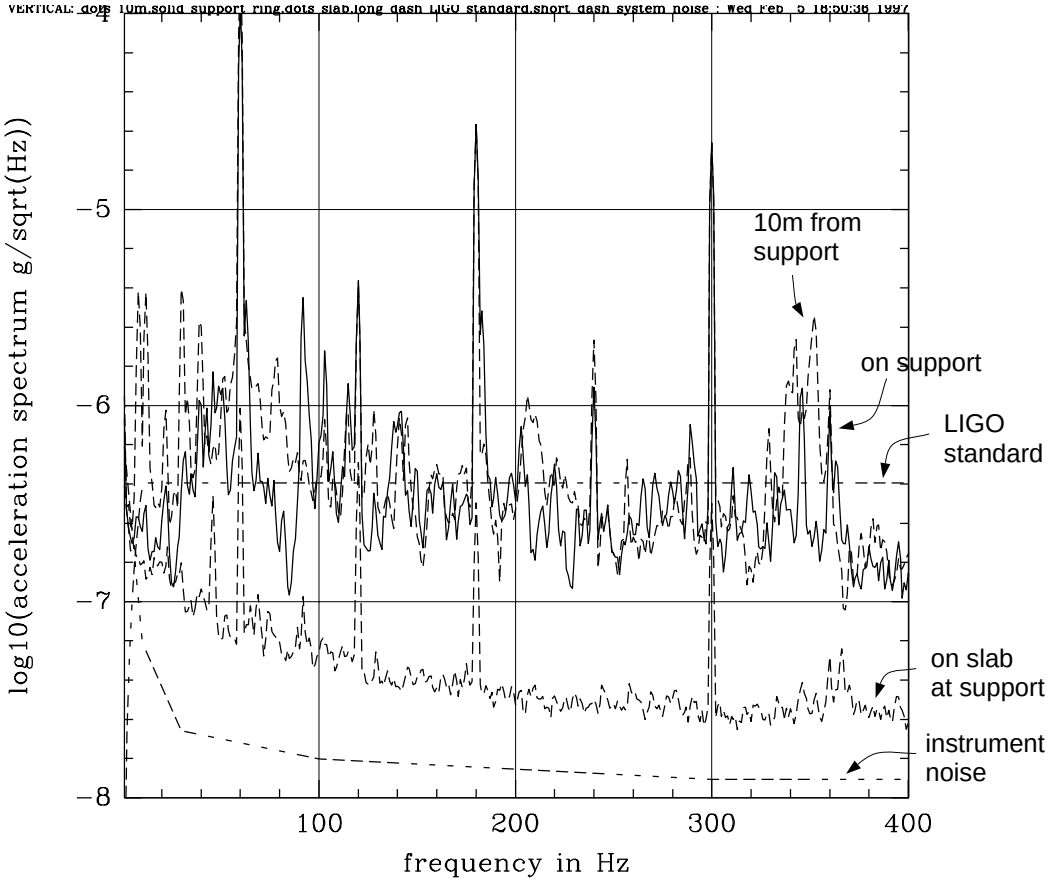

Figure 3 Vertical acceleration spectrum

All the spectra taken on the tube are poorly correlated with the acceleration spectra taken near the slab and (as was discovered later) are well correlated with the acoustic pressure spectra measured on a microphone placed near the accelerometer on the tube. The motion of the tube implies a driving sound field of 25 to 30 db (3 to 6 x 10^{-3} dynes/cm^2 rms) , just below audible in the 100 Hz band, which is consistent with our observations that it was really quiet (as quiet as the proverbial church crypt) while taking the measurements. The acoustic noise is expected to vary as the square of the wind velocity so that under more typical conditions of 10 mph wind velocities, the acceleration noise may increase by a factorof 4. This factor is consistent with daytime measurements but not well defined since besides increased wind there was increased activity on the road to the Hanford facilities as well as CB&I construction.

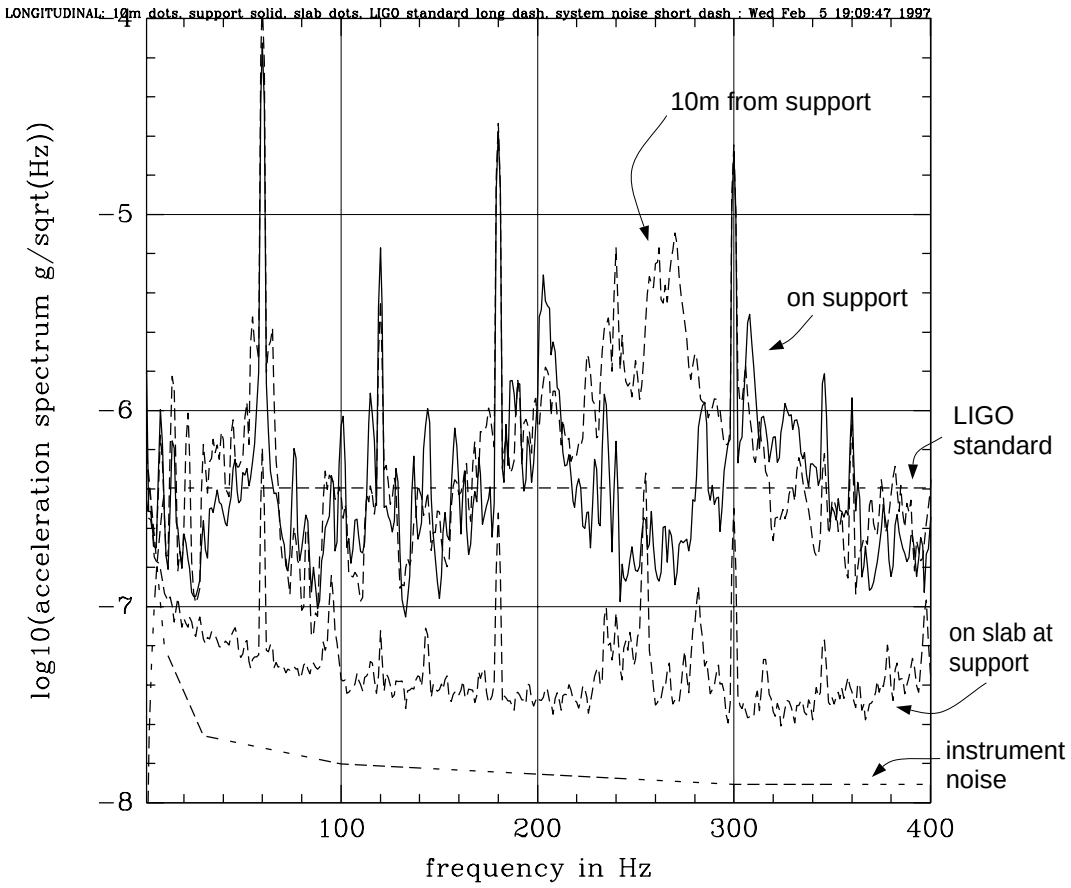

Figure 4 Longitudinal acceleration spectrum

Acoustic transfer functions. Figures 5, 6 and 7 show the calibrated transfer functions of beam tube acceleration in g for acoustic pressure in dynes /cm^2 measured next to the accelerometer by a microphone (calibrated after the fact). The accelerometer was located mid tube 10 meters from the fixed support and oriented for horizontal, vertical and longitudinal motions sequentially. The sound source was a loudspeaker mounted at the beam tube enclosure door (the outside world acting as an infinte baffle). There is little random noise in the figures since the excitation was made large enough to override the ambient background. The scruffy appearance of the data is due to the complexity of the beam tube normal mode structure.

The large scale interaction of the beam tube with the acoustic field is described by P.M. Morse in *Vibration and Sound* Mc Graw Hill (1948) p 352. The scale parameter for the process is the ratio

$$\mu = \frac{2\pi a}{\lambda} = \frac{2\pi a f}{c}$$

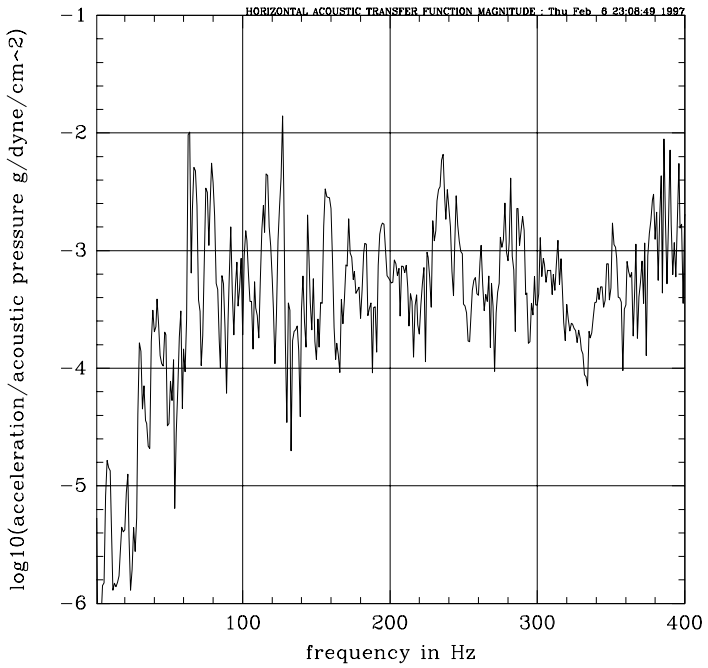

Figure 5 Acoustically driven horizontal acceleration

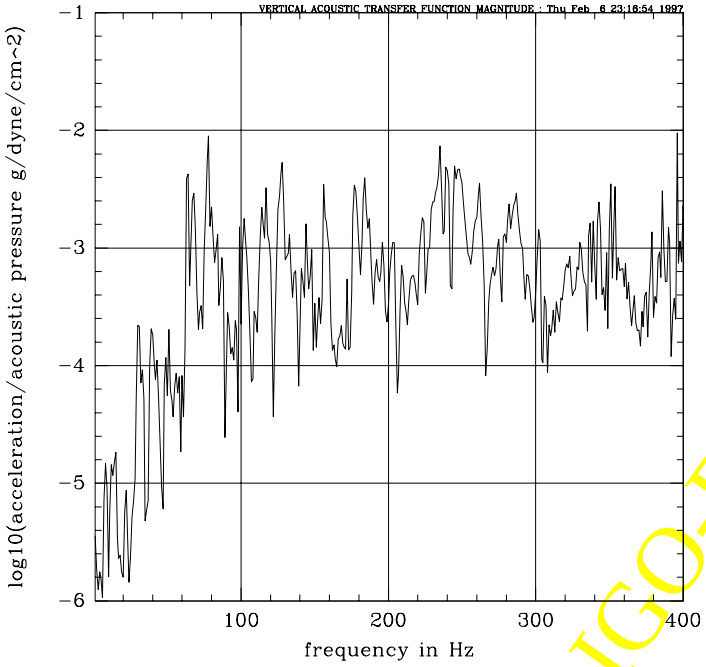

Figure 6 Acoustically driven vertical acceleration

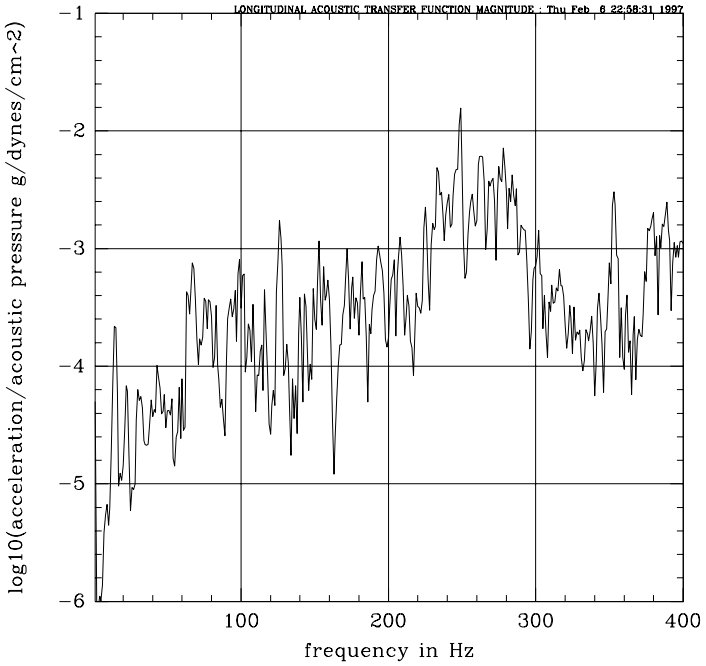

Figure 7 Acoustically driven longitudinal acceleration

where a is the tube radius, c the speed of sound in air and f the acoustic frequency. The scale factor becomes unity at about 85 Hz. At lower frequencies the tube acceleration in units of g per acoustic pressure grows linearly with frequency and is given by

$$\frac{(acc)/g}{p} = \frac{2\pi af}{c\rho_{ss} tg}$$

where ρ_{ss} is the density of the stainless steel, t the thickness of the tube wall modified for the stiffening rings. At frequencies above 85 Hz the sound diffraction is less important and the acceleration of the tube per acoustic pressure decreases slowly with frequency as

$$\frac{(acc)/g}{p} = \frac{1}{\pi g t \rho_{ss}} \sqrt{\frac{c}{2af}}$$

The crude model gives 3 x 10^{-4} g/dyne/cm^2 at a 100 Hz possibly fortuitous in its good agreement with the data.

We failed in our measurement of the acoustic transmission of the beam tube enclosure and in subsequent measurements at the site it would be useful to measure this quantity as a function of frequency. An approximate relation for the acoustic transmission loss of a sheet of material between 125 to 4000 Hz is given in the American Institute of Physics Handbook (p 3-150) as a function of the material mass per unit area $\sigma = \rho_{mat} t$,

$$db_{att} = 12.7 + 14.7 \log \sigma (\mathrm{kg/m^2})$$

Using the above expression the 6 inch thick beam tube enclosure would provide about 50 db of acoustic noise reduction. The 6 inches of insulation to be placed on the tube for the bake is expected to provide about 20 db of isolation at frequencies above 200 Hz but be ineffective at frequencies below 100Hz.

The simple geometry of the beam tube enclosure is amenable to active acoustic noise reduction (closed loop nulling systems of microphones and loudspeakers) that have been developed for noise reduction in ducts. This may be a promising direction to take if advanced interferometer systems require further reduction in the beam tube motions.

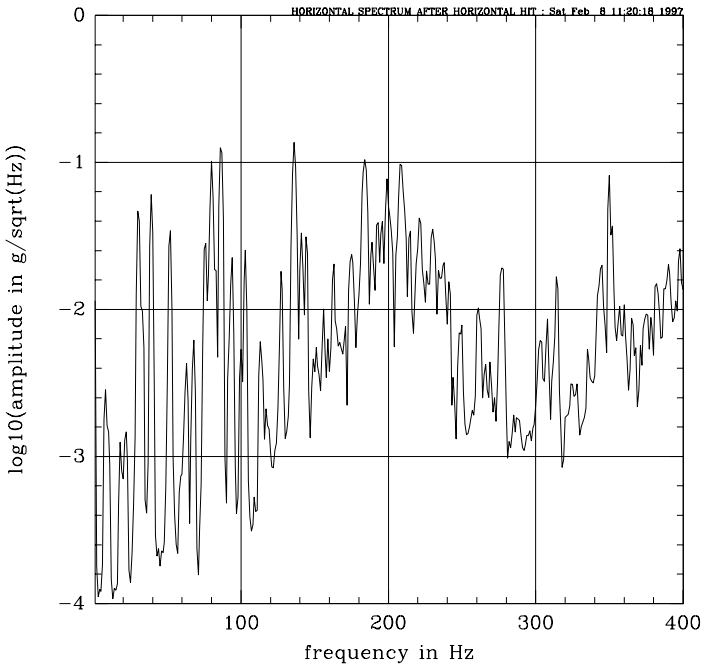

Figure 8 Horizontal transient spectrum after horizontal impulse

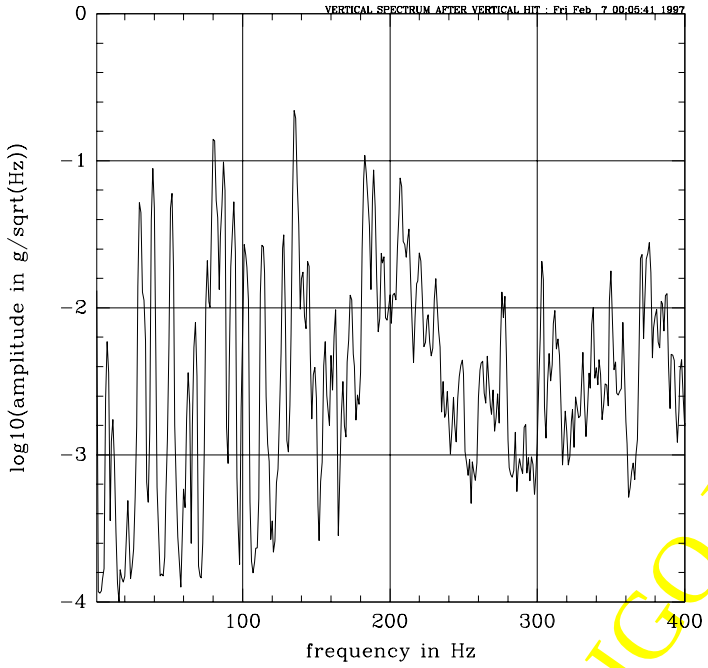

Figure 9 Vertical transient spectrum after vertical impulse

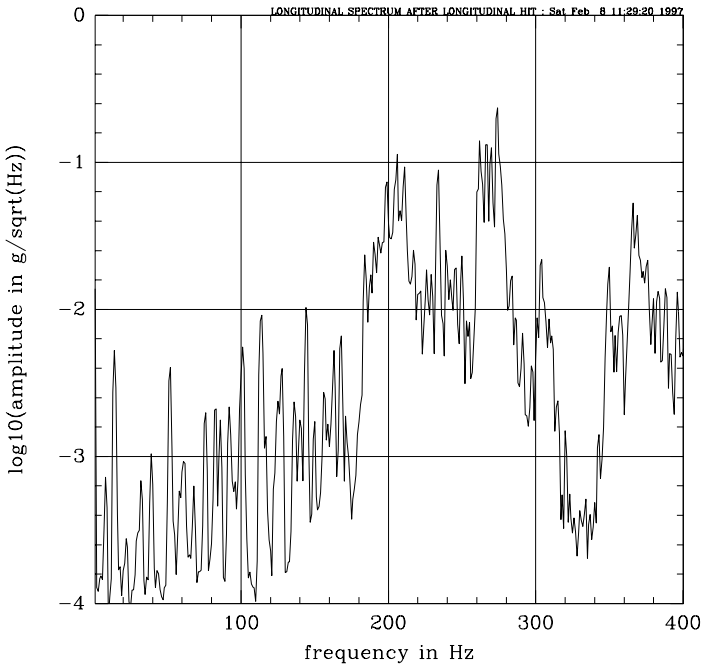

Figure 10 Longitudinal transient spectrum after longitudinal impulse

Transient measurements The ringdown spectrum after an impulse to the beamtube by a wooden hammer is shown in Figures 8, 9 and 10. A compilation of the normal mode frequencies for the three orthogonal directions of motion is given in table 1. All the measurements were made by mounting the accelerometer on a stiffening ring at the midpoint of the tube. The impulse was given at the fixed support in the direction indicated in the figure caption. The normal mode peak widths in the figures are determined by the observation time rather than the intrinsic normal mode losses. All resonances are narrower than 1Hz. The ringdown time of several of the higher frequency modes was measured directly. The several of the modes between 300 to 400 Hz (stiffening ring radial modes coupled by the beamtube shell) have a ringdown time of 2 seconds, the Q of some of these modes is over 1000. The Q of the 87 Hz transverse mode is about 400. The thermal insulation needed for the bakeout should provide enough damping to reduce the Q to below 100 for all the modes with frequency higher than 50Hz.

We should have taken high resolution spectra commensurate with line widths equal to the normal mode widths when evaluating the noise. The error in the peak heights will at most be a factor of 2 while the area (the broad band excitation) is correctly described. The insulation will bring the peak heights to the values in figures 2,3 and 4.

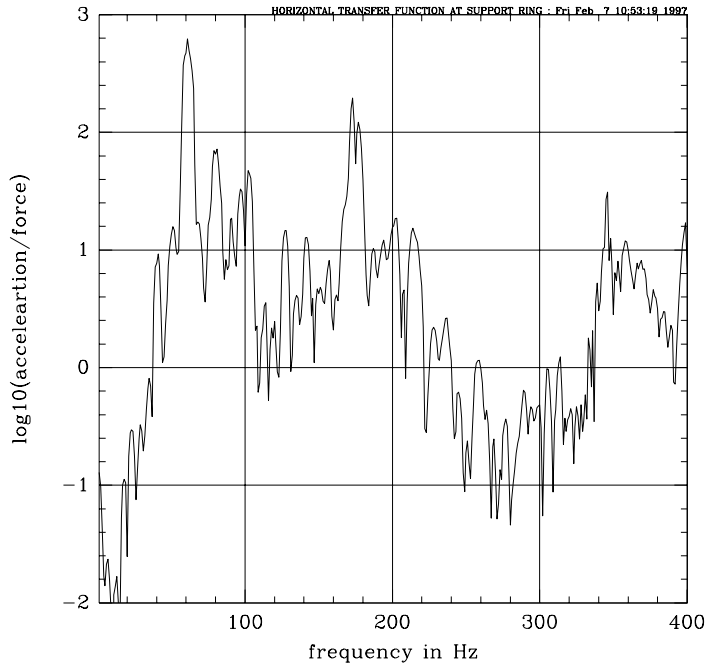

Figure 11 Horizontal acceleration for horizontal excitation

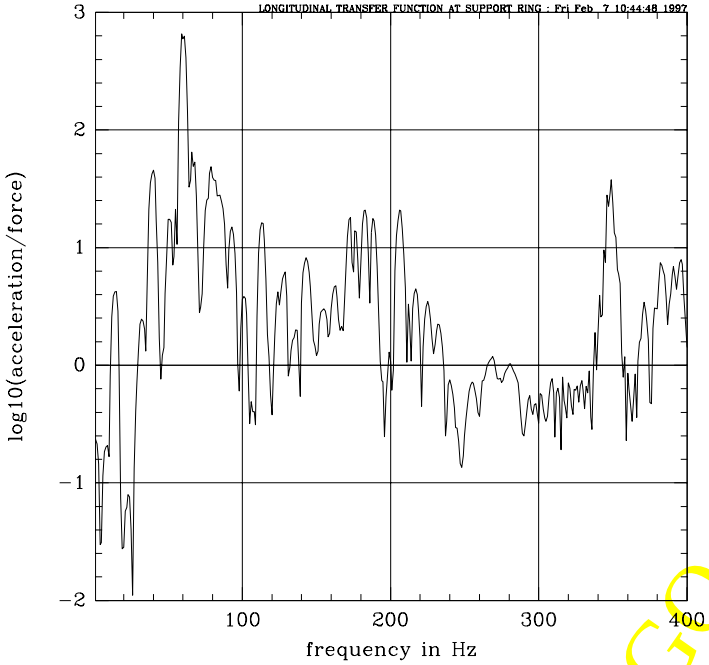

Figure 12 Longitudinal acceleration for longitudinal excitation

Driven measurements Figure 11 and 12 show the transfer functions of acceleration to force with a swept sine excitation. The force was applied to the beam tube by a magnet attached to the tube driven by the current in a coil which was held to the ground. The curves have been corrected for the inductance of the coil since the system was driven from a voltage source. The accelerometer was placed at the fixed support and the driver on a stiffening ring. The data has been included in the report for completeness but has not been used in the analysis.

Table 1: Normal mode frequencies in Hz

vert freq	strength	horiz freq	strength	long freq	strength
8	st	8		8	
12		18		14	
17		22		22	
22		30	st	32	
30	st	39	st	39	
39	st	52	st	52	
52	st	63		61	
60		68		68	
63		76	st	76	
68		80	st	83	
76	st	82	st	92	
80	st	86	st	101	
87	st	94	st	114	st
94	st	100		128	
101	st	103	st	136	
113	st	109		140	
128	st	113		144	st
135	st	127	st	150	
141	st	136	st	156	
144	st	141	st	163	
156		144	st	168	
163		149		184	st

Table 1: Normal mode frequencies in Hz

vert freq	strength	horiz freq	strength	long freq	strength
168		156	st	188	st
173	st	159		190	st
183	st	163	st	193	st
189	st	175	st	199	st
194	st	184	st	206	st
196	st	189	st	211	st
200	st	193	st	217	st
207	st	196	st	222	st
213	st	199	st	226	st
220	st	208	st	234	st
226		221	st	239	st
231	st	230	st	246	st
236		234	st	250	st
243		238	st	253	
249		241	st	262	st
254		250		267	st
263		261	st	270	st
270		266		274	st
276	st	269		284	st
278	st	278	st	291	
285		303		297	
292		308		301	
303	st	314	st	304	st
312		324		320	
319		325		330	
324		345	st	334	
331		350	st	343	

Table 1: Normal mode frequencies in Hz

vert freq	strength	horiz freq	strength	long freq	strength
335		357	st	350	st
338	st	360		354	
342		365		358	st
350	st	371		366	st
358		375		369	st
371	st	378		376	st
376	st	382	st	380	st
381		390	st	383	st
384	st	395	st	388	st
388	st	398	st	396	st
398					